Effect of perturbation timing on recovering whole-body angular momentum during very slow walking

van Mierlo, M.; Abma, M.; Vlutters, M.; van Asseldonk, E. H.F.; van der Kooij, H.

DOI
10.1016/j.humov.2023.103138

Publication date
2023

Document Version
Final published version

Published in
Human Movement Science

Human Movement Science 91 (2023) 103138

Contents lists available at ScienceDirect

Human Movement Science

journal homepage: www.elsevier.com/locate/humov

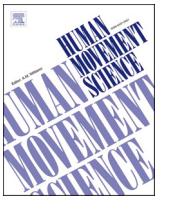

Effect of perturbation timing on recovering whole-body angular momentum during very slow walking

M. van Mierlo [a,*], M. Abma [a], M. Vlutters [a], E.H.F. van Asseldonk [a], H. van der Kooij [a,b]

[a] Department of Biomechanical Engineering, University of Twente, Enschede, The Netherlands
[b] Department of Biomechanical Engineering, Delft University of Technology, Delft, The Netherlands

ARTICLE INFO

Keywords:
Human balance
Gait
Very slow walking
Whole-body angular momentum
Centre of pressure modulation
Ground reaction force vector

ABSTRACT

Humans prioritize regulation of the whole-body angular momentum (WBAM) during walking. When perturbed, modulations of the moment arm of the ground reaction force (GRF) with respect to the centre of mass (CoM) assist in recovering WBAM. For sagittal-plane perturbations of the WBAM given at toe off right (TOR), horizontal GRF modulations and not centre of pressure (COP) modulations were mainly responsible for these moment arm modulations. In this study, we aimed to find whether the instant of perturbations affects the contributions of the GRF and/or CoP modulations to the moment arm changes, in balance recovery during very slow walking. Perturbations of the WBAM were applied at three different instants of the gait cycle, namely at TOR, mid-swing (MS), and heel strike right (HSR). Forces equal to 16% of the participant's body weight were applied simultaneously to the pelvis and upper body in opposite directions for a duration of 150 ms. The results showed that the perturbation onset did not significantly affect the GRF moment arm modulation. However, the contribution of both the CoP and GRF modulation to the moment arm changes did change depending on the perturbation instant. After perturbations resulting in a forward pitch of the trunk a larger contribution was present from the CoP modulation when perturbations were given at MS or HSR, compared to perturbations at TOR. After backward pitch perturbations given at MS and HSR the CoP modulation counteracted the moment arm required for WBAM recovery. Therefore a larger contribution from the horizontal GRF was needed to direct the GRF posterior to the CoM and recover WBAM. In conclusion, the onset of WBAM perturbations does not affect the moment arm modulation needed for WBAM recovery, while it does affect the way CoP and GRF modulation contribute to that recovery.

1. Introduction

The whole-body angular momentum (WBAM), a concept describing the body's rotational motion, is highly regulated and prioritized in human walking (Herr & Popovic, 2008; van Mierlo, Ambrosius, Vlutters, van Asseldonk, & van der Kooij, 2022). Segment-to-segment angular momentum cancellations minimize deviations of the WBAM during unperturbed walking (Herr & Popovic, 2008; Robert, Bennett, Russell, Zirker, & Abel, 2009; Negishi & Ogihara, 2023). Furthermore, when perturbed, a highly prioritised and efficient strategy is used for WBAM recovery (van Mierlo et al., 2022; Schumacher et al., 2019). Schumacher et al. (2019) developed a

* Corresponding author.
E-mail address: m.vanmierlo@utwente.nl (M. van Mierlo).

https://doi.org/10.1016/j.humov.2023.103138
Received 7 April 2023; Received in revised form 29 June 2023; Accepted 4 August 2023
Available online 11 August 2023

method to apply net moments to the trunk perturbing the WBAM during standing, without affecting the whole-body linear momentum (WBLM). They demonstrated a quick recovery that restored upper-body balance. Studying the balance responses to perturbations of the WBAM and WBLM separately helps to better understand the contributions of different recovery strategies in daily-life situations.

Our previous study on balance regulation during walking (van Mierlo et al., 2022) also shows that WBAM disturbances result in a quick recovery to minimize the deviation from the WBAM at perturbation onset. The stance leg hip joint provides an important contribution to this recovery by changing the direction of the ground reaction force (GRF). This introduces a moment arm of the GRF with respect to the whole-body centre of mass (CoM). In the rest of this article this moment arm will be referred to as the 'GRF moment arm'. Changes in this GRF moment arm can help to correct for WBAM perturbations given at toe-off (van Mierlo et al., 2022). Since the use of this strategy goes at the expense of WBLM regulation, it emphasizes the importance of WBAM control in human walking. A better understanding of WBAM recovery may aid in the development of rehabilitation training and balance controllers for assistive devices (Schumacher et al., 2019; van Mierlo et al., 2022).

In van Mierlo et al. (2022) we applied sagittal-plane perturbations of the WBAM only at toe-off right (TOR). Yet, the available options for balance recovery and the risks that come with a balance disturbance are dependent on the body posture (Weerdesteyn, Laing, & Robinovitch, 2012; Hof, Vermerris, & Gjaltema, 2010; Vlutters, van Asseldonk, & van der Kooij, 2018), which changes throughout the gait cycle. Responses in terms of foot placement adjustments after mediolateral (ML) perturbations of the WBLM have shown to change depending on the perturbation onset timing, since some time is needed in order to adjust foot placement (Hof et al., 2010; Vlutters et al., 2018). For similar perturbations in anteroposterior (AP) direction, foot placement turned out to be less dependent on the perturbation onset timing (Vlutters et al., 2018; Leestma, Golyski, Smith, Sawicki, & Young, 2023). However, for stumbling perturbations and slip-like perturbations, affecting both the WBLM and WBAM, the onset did affect the recovery strategy (Forner Cordero, Koopman, & van der Helm, 2003; Eveld, King, Vailati, Zelik, & Goldfarb, 2021; Golyski, Vazquez, Leestma, & Sawicki, 2022). In stumbling, a blockage during early swing results in an elevation strategy, while for perturbations given later during swing this shifts towards a lowering strategy of the leg (Forner Cordero et al., 2003; Eveld et al., 2021). For slip-like perturbations, a late-swing onset of a treadmill belt acceleration resulted in larger stabilizing responses directly after the perturbations in terms of an increased step length and margin of stability compared to perturbation onsets during early-swing (Golyski et al., 2022). This suggests that the balance response is affected by the perturbation onset timing when both the WBLM and WBAM are disturbed. However, it is unknown whether this also occurs for perturbations that mainly affect the WBAM, but not the WBLM.

To increase the fundamental understanding of WBAM recovery we aimed to find whether balance responses to WBAM perturbations depend on the instant of the gait cycle at which they were given. This is studied during a very low walking speed, as in Zadravec et al. (2020), since this better relates to individuals suffering from balance problems and to whom the knowledge on human balance control strategies is relevant for improving rehabilitation training and balance assistance (Nymark, Balmer, Melis, Edward, & Millar, 2005). Studying balance responses during very slow walking makes the results better applicable within these fields, since very slow walking affects gait characteristics and the opportunities for balance recovery, which are hard to extrapolate from studies at normal walking speeds (Wu, Simpson, van Asseldonk, van der Kooij, & Ijspeert, 2019; van Mierlo, Vlutters, van Asseldonk, & van der Kooij, 2023). Previous research has shown a main contribution of GRF direction modulations to the change in GRF moment arm in order to recover from WBAM perturbations given at TOR (van Mierlo et al., 2022) (Fig. 1a). Perturbations given at other instants of the gait cycle also require GRF moment arm modulations for WBAM recovery. However, we hypothesize that a centre of pressure (CoP) modulation also contributes to achieving these GRF moment arm adjustments (Fig. 1b), because: (1) The double support phase gives large opportunities for CoP modulation (van Mierlo, Vlutters, van Asseldonk, & van der Kooij, 2021). Therefore, for perturbations

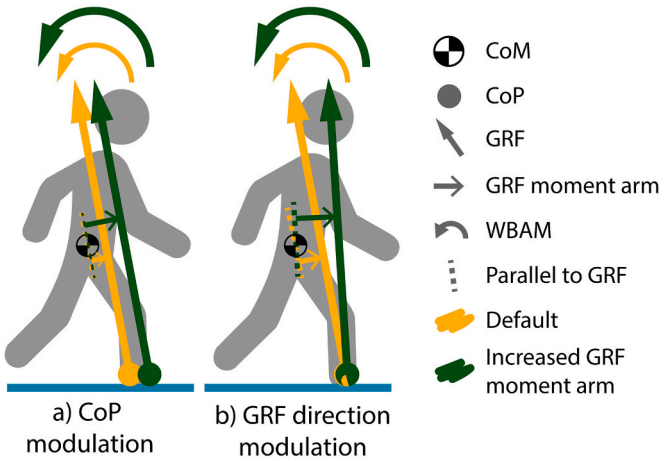

Fig. 1. GRF moment arm modulation. (a) and (b) present methods to affect the GRF moment arm by either modulating the CoP or GRF direction respectively. A default scenario of the GRF vector is presented in yellow with the resultant moment arm between the GRF vector and a parallel line through the CoM. The green line presents an example of a modulation in either the CoP (a) or GRF direction (b), both increasing the GRF moment arm.

given just before or during the double support phase a larger contribution is expected from CoP modulations. (2) According to the foot placement estimator (FPE), adjustments in the CoP position are needed in order to regulate a constant offset control in case of a WBAM disturbance (Millard, Wight, McPhee, Kubica, & Wang, 2009). The FPE estimates where to place the CoP in order to come to a halt or continue walking, based on the WBLM and WBAM. For perturbations given late during single support, the WBAM will still be disturbed at the moment of heel contact, according to the FPE this likely results in a foot placement modulation affecting the CoP position and assisting in the recovery. Overall it is expected that for perturbations given later during the swing phase or during double support, both the CoP and GRF direction modulations substantially contribute to the GRF moment arm changes for, while for perturbations given at the beginning of the swing phase this mainly originates from GRF modulation.

2. Methods

2.1. Participants

Ten healthy volunteers participated in this study (six female, age 24 ± 3 year, weight 66 ± 10 kg, height 1.75 ± 0.10 m, mean pm std). The local ethics committee of the University of Twente approved the experimental protocol and setup (reference number RP 2019–88). Before starting the experiment, all participants gave written informed consent in accordance with the Declaration of Helsinki.

2.2. Setup

The same experimental setup was used as in van Mierlo et al. (2022). The experiments were performed on a dual-belt treadmill with build-in force plates beneath each belt (custom Y-Mill, Motekforce Link, The Netherlands). Two motors (SMH60, Moog, The Netherlands) behind the treadmill were used to apply the perturbations to the pelvis and upper body. Horizontal rods were connected to the participant's body via a brace worn around the pelvis and upper body. Load cells were integrated in the horizontal rods to measure and minimize the interaction forces with the participant via an admittance controller (described in van der Kooij et al. (2022)), except when a perturbation was given. At that instant the controller had to track a desired force different from zero. The participants wore a safety harness connected to a fall protection system at the ceiling. The height of the motors was adjusted based on the height of the participant. The motor applying perturbations to the pelvis was placed such that the horizontal rod had a height matching the pelvis height of the participant, resulting horizontal rod height ranging from 0.96 m till 1.05 m. The motor applying perturbations to the upper body was placed 0.40 m higher compared to the motor for the pelvis perturbations, resulting in a height within the range from 1.36 m till 1.45 m. By using these two motors to give two simultaneous perturbations in opposite direction, this setup enabled the ability to apply perturbations of mainly the WBAM.

2.3. Data collection

Eight Qualisys cameras (Oqus 600+, Qualisys, Göteborg, Sweden) were used to record the kinematic data. The data of the following reflective markers was recorded at 128 Hz via Qualisys Track Manager (QTM): 10 rigid bodies with 4 markers each were placed on the sternum, pelvis, upper legs, lower legs, upper arms and forearms respectively. A total of 35 single markers were placed on the participant: 3 markers on the head (on a headband: 1 on the frontal side in the middle and 2 on the left and right side above the ear) and the left and right calcaneus, 1st and 5th metatarsal heads, medial and lateral malleoli, medial and lateral epicondyles of the femur, anterior and posterior superior iliac spines, acromia, medial and lateral humeral epicondyles, ulnar and radial styloids, and the 2nd and 5th metacarpal heads. This marker set was adjusted from the set used in Rajagopal et al. (2016). Data from the force plates was recorded at 2048 Hz in sync with the motion capture data via an analog interface. Data from the computer controlling the motors for the perturbations was recorded at 1000 Hz and synchronised with the other data via a synchronisation signal.

2.4. Experimental protocol

The experiment comprised four blocks. The first block consisted of unperturbed walking for 3 minutes to familiarize with treadmill walking. The very low walking speed was 0.44 m s^{-1}, scaled as following: walking speed (ws) $= 0.44 \cdot \sqrt{l}$, with l measured from the floor to the trochanter major while standing straight. After this, three blocks followed in which perturbations were applied. These perturbations consisted of two simultaneous perturbations in opposite directions to the upper body and pelvis, with a magnitude of 16% of the participant's body weight for a duration of 150 ms. These perturbations have shown to be effective on the WBAM (van Mierlo et al., 2022). Forward perturbations to the pelvis together with backward perturbations to the upper body are called backward pitch perturbations (BPP). Backward pelvis perturbations together with forward upper body perturbations are called forward pitch perturbations (FPP). The difference between the three blocks was the instance at which the perturbation was given. The perturbations were either given at TOR, mid-swing (MS) with left being the stance leg or at heel strike right (HSR). Based on Matjacic, Zadravec, and Olenšek (2020) we did not expect effects of selecting either the dominant or non-dominant leg to be the stance leg at the perturbation instant. The order of these blocks was randomized among the participants. Real-time gait phase detection based on the GRF data was used to identify the instances at which the perturbations were given. TOR was defined as the instant at which the vertical GRF of the right belt came below 5% of the participant's body weight. HSR was defined as the instant at which the vertical GRF of the right belt

came above 5% of the participant's body weight. The first walking block without perturbations was used to measure the average duration of the single support phase left. For the perturbations given at MS a participant-specific offset of half the average duration of the single support phase left was used from the instant of TOR. Ten repetitions of each perturbation direction (BPP and FPP) were given in each perturbation block, resulting in 20 perturbations per block. The back- and forward pitch perturbations were given in a randomized order with a random interval ranging from 4 to 7 strides in between. The participants were instructed to walk with their arms along their body with a natural arm swing and without grasping the railing.

2.5. Data processing

The data processing was similar to the one described in van Mierlo et al. (2022). The QTM software was used for labelling of the markers and interpolation of the missing samples, using the polynomial and relational gap filling tool. Further data processing was done with Matlab (R2022a, MathWorks). A 6th order zero phase low pass Butterworth filter with a cut off frequency based on the participant's cadence ($cadence \cdot 6.25\ Hz$) was used to filter the marker and force data (Rácz & Kiss, 2021). For each participant a 22 segment full body model (Rajagopal et al., 2016), containing 3 additional markers on the head, was scaled in OpenSim 4.3 (Delp et al., 2007). Sagittal-plane orientations and angular velocities of the individual segments and the CoM positions and velocities of the individual segments and the whole body were obtained using the OpenSim analyze tool. The inverse dynamics tool was used to obtain the joint moments around the ML axis. The GRF and moment measurements were used to acquire the horizontal GRF component and to calculate the CoP position, expressed relative to the vertical projection of the whole-body CoM. The GRF moment arm was calculated with respect to the CoM position in the sagittal-plane. The WBAM was calculated with Eq. (1), where i presents each body segment of the OpenSim model, $\vec{r}^{\,i}_{CoM}$ and $\vec{r}_{CoM}$ the position of each i-th segment and the whole body CoM respectively in the sagittal plane, m_i each i-th segment's mass, $\vec{v}^{\,i}_{CoM}$ and $\vec{v}_{CoM}$ the velocity of each i-th segment and the whole body CoM respectively in the sagittal-plane, I^i each i-th segment's inertia tensor (obtained from the OpenSim model), and ω^i the angular velocity about the i-th segment's CoM (Herr & Popovic, 2008). All measures are given in the global frame and in the sagittal-plane or about the ML axis.

$$H = \sum_{i=1}^{22}[(\vec{r}^{\,i}_{CoM} - \vec{r}_{CoM}) \times m_i(\vec{v}^{\,i}_{CoM} - \vec{v}_{CoM}) + I^i\omega^i] \tag{1}$$

All measures were scaled for the individual participants by dividing through a scaling factor based on the participant's leg length (l), mass (m), height (h), and/or ws making the values dimensionless: $WBAM \rightarrow m \cdot h \cdot ws$; $velocity \rightarrow \sqrt{g \cdot l}$; $position \rightarrow l$. To bring the values back to the original order of magnitude, the scaled measures were multiplied with the measure-specific scaling factor calculated from the averages across all participants. All measures were also normalized over time by resampling each (gait) phase to 50 samples, synchronizing the instants of toe-off, heel strike, and the start and end of the perturbation. This allowed for averaging the data over all repetitions within each participant and across all participants. For the presentation in the figures, the time normalised data of the average responses were brought back to the original time scale using the participant-specific average gait phase durations.

2.6. Outcome measures

The effect of the perturbation on the gait phase duration was expressed by the change in gait phase duration with respect to the gait phase duration during unperturbed walking. This was measured for the first single and double support phase. To quantify the response, outcome measures were defined, being the maximal deviation of a measure due the perturbation with respect to unperturbed walking. For the WBAM and CoM velocity the maximal deviation was taken between the onset of the perturbation and 160 ms after, to quantify the effect of the perturbation. For the other measures, which are the GRF moment arm, the CoP position with respect to the CoM, the horizontal GRF, and the joint moments of the left and right hip, knee and ankle, the maximum deviation was taken between the perturbation onset and first 300 ms after. This range was selected because the main response occurs within this time frame. The exact instances at which the measures were taken differ for the different perturbation directions and outcome measures.

2.7. Statistics

Linear mixed models were used to evaluate the dependence of the outcome measures on the instant of the perturbations using R4.1.2 (R Core Team, 2021, Vienna, Austria). The perturbation instants were added to the model as a categorical fixed effect. Random effects for the intercept and slope were included to take the participant effect into account. The main effects were tested with a significance level of $\alpha = 0.05$ using the Wald t-test with a Kenward-Roger correction for the degrees of freedom. The intercept revealed whether there was a significant offset, indicating a significant response due to the perturbation. The significance of the parameter estimates revealed whether there was a significant difference between the perturbation onsets. This could result in cases were there is an uncertainty about the perturbations conditions resulting in a significant difference from the unperturbed condition, since the offset value and parameter estimate could cancel each other. In these cases an additional one-sample t-test was performed for the concerning perturbation condition. A Bonferroni correction was applied to correct for the multiple t-tests that were performed. Ten additional t-tests had to be performed because of this uncertainty. Therefore, the significance was tested with a level of $\alpha = \frac{0.05}{10} = 0.005$.

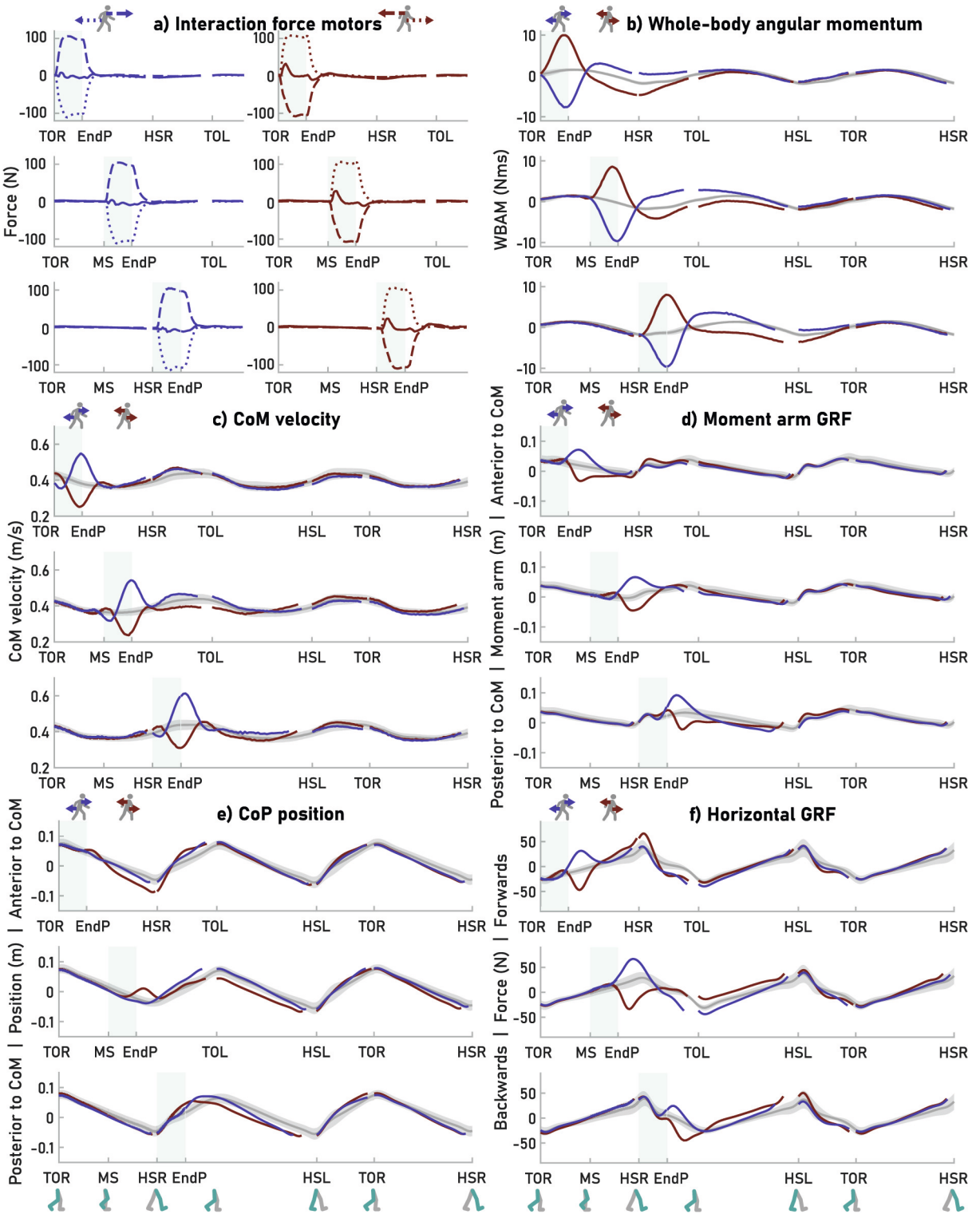

(caption on next page)

Fig. 2. Time series perturbation effect. Averaged time series presenting (a) interaction forces between the motors and the participants with the force between the motor and the pelvis presented with a dotted line and with the upper body with a dashed line. The summed forces are presented with the continuous line. On the left the forces for the FPP and on the right for the BPP. (b) The WBAM about the ML axis, (c) the CoM velocity, (d) the moment arm of the GRF with respect to the CoM in the sagittal plane, (e) the AP CoP position with respect to the CoM and (f) the horizontal GRF from TOR until the second HSR. Each subfigure contains the results for perturbations given at TOR (top-graph), MS (middle-graph), and HSR (bottom-graph). The shaded area indicates the duration the perturbation was given. The unperturbed condition is presented in gray together with the standard deviation, FPP are presented in blue and BPP in red. The graphs are time synchronised at each gait event.

3. Results

3.1. Perturbation effect

Data analysis showed that not all perturbations were given at the intended instant. Perturbations that were not given at the correct instant were removed from further analysis. This was the case for 7.2% of the perturbations (0.8% for perturbation onset at TOR, 2.4% for MS and 4.0% for HSR). The sums of the interaction forces between the motors and the participants pelvis and upper body approximate zero, Fig. 2a.

As intended, the back- and forward pitch perturbations significantly affected the WBAM (Figs. 2b and 4a and Table A1). The absolute maximal WBAM deviation due to the perturbation was similar for the different perturbation directions (−9.85 N m s for FPP and 9.17 N m s for BPP), except for those given at HSR. For the FPP given at HSR the maximal WBAM deviation was significantly smaller compared to the other perturbation onsets (−8.64 N m s). Still the response was significantly different from the unperturbed condition. For the BPP at HSR the maximal WBAM deviation was significantly larger (9.83 N m s) compared to the other perturbation onsets. The perturbations also significantly affected the maximal CoM velocity deviation (0.168 m s^{-1} for FPP and −0.151 m s^{-1} for BPP), without a noticeable difference between the various perturbation onsets (Figs. 2c and 4b and Table A1.).

3.2. GRF moment arm, CoP and GRF modulation

The GRF moment arm modulation after the perturbations results in a moment about the CoM that helps in recovering the perturbed WBAM (Fig. 2d). For the FPP this entailed a GRF passing anterior to the CoM and for the BPP a moment arm passing posterior to the CoM. For both the back- and forward pitch perturbations there was no significant difference for the different perturbation onset timings in the maximum deviation of the GRF moment arm with respect to the unperturbed condition (Fig. 4c, Table A1).

Two important measures affecting the GRF moment arm, the CoP position and horizontal GRF, differed for the different perturbation onset timings. For the BPP, all the different perturbation onset timings had a significant effect on the maximal CoP deviation (Fig. 2e and Table A1). For the perturbations given at TOR, the CoP was kept more posterior with respect to unperturbed walking, this contributed to having the GRF directed posterior of the CoM. However, for the perturbations given at MS and HSR, the CoP was placed more anterior compared to unperturbed walking, which counteracts having the GRF pass posterior from the CoM. For the BPP given at MS the horizontal GRF corrected for this counteracting CoP position, since a significant larger change in the horizontal GRF was present after these perturbations compared to the other perturbation instants (Fig. 2f and Table A1).

After FPP the horizontal GRF significantly increased, assisting in obtaining the GRF moment arm needed for recovery. The different perturbation timings did not significantly affect the size of the change in the horizontal GRF. Only the perturbations given at HSR had a significant effect on the CoP (Fig. 2e and Table A1). The more forward positioned CoP contributes to directing the GRF anterior to the CoM. Fig. 2e and f suggests that for FPP given at HSR, a larger contribution is present from the CoP modulation, while the change in horizontal GRF decreases.

3.3. Gait phase durations

The average time spend in single support decreased due to the perturbations, except for BPP given at TOR (Fig. 4f and Table A1). This effect was not significant due to the large variation among the participants. The time spend in double support did decrease significantly for all perturbation conditions (Fig. 4g and Table A1).

3.4. Joint responses

The different perturbation onset timings affected the joint contributions from the left and right leg (Fig. 3 and Table A1). For perturbations given at TOR, the left ankle, knee and hip joints, which is the stance leg, significantly contributed to the recovery, except for the left ankle joint after the FPP (Fig. 4). The hip flexion together with knee extension in case of a BPP and the hip extension together with knee flexion in case of a FPP assist in recovering the WBAM disturbance. The joints of the right leg, the leg in swing at that time, did not significantly contribute (Fig. 4). This changed for perturbations given at MS or HSR. For the perturbations given at MS most joints of both legs were significantly involved in the recovery. For the perturbations given at HSR the largest responses were seen in the leading leg (in this case the right leg), but the hip and ankle joint of the trailing leg were still significantly involved in the response as well. Overall the contribution of the ankle joints appeared to be smaller compared to the knee and hip joints. After both the back- and forward pitch perturbations the plantarflexion moment of the left ankle decreased, while for the right leg the plantarflexion moment increased for FPP given at MS and HSR and only decreased after BPP at HSR.

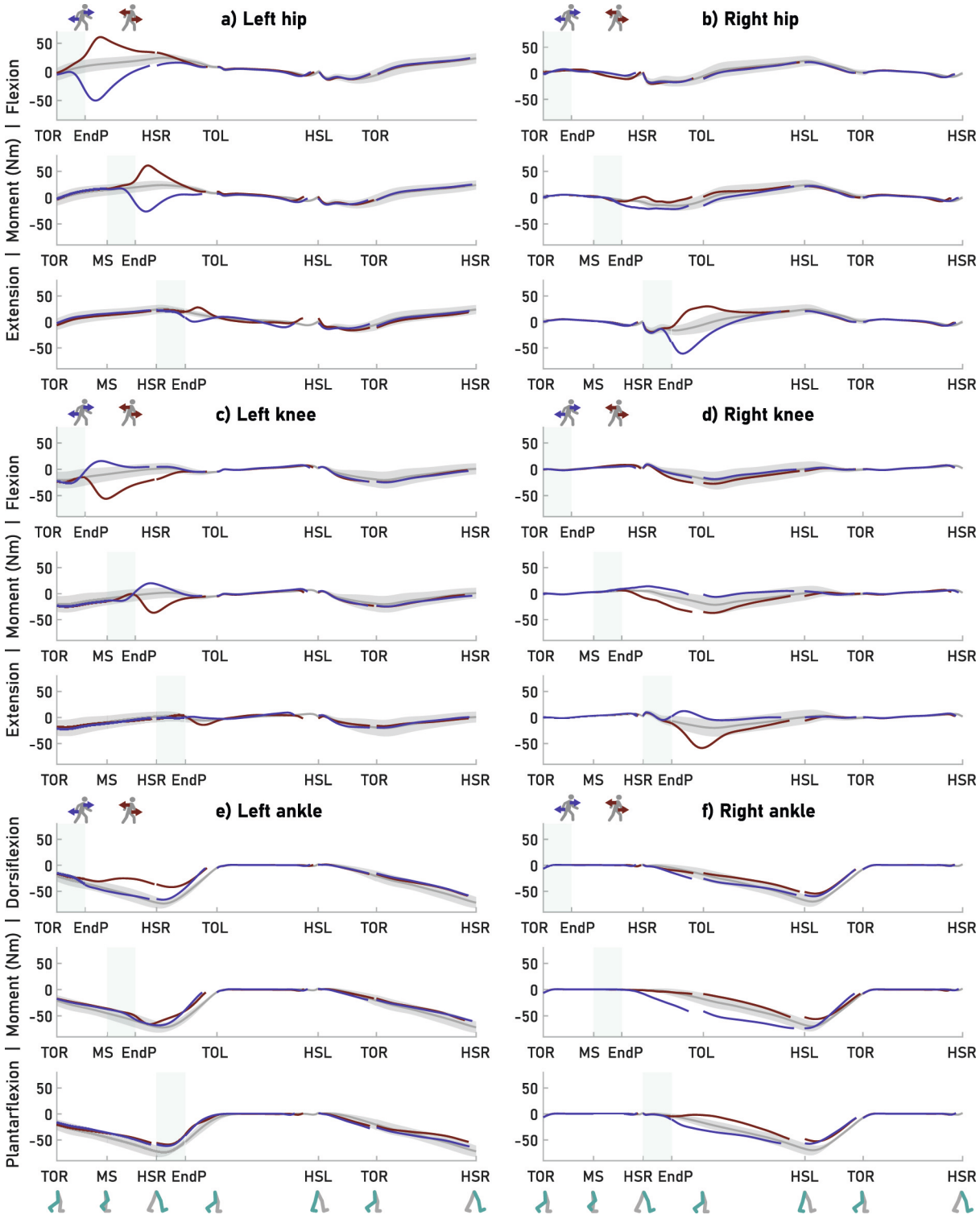

Fig. 3. Time series joint moments perturbation effect. Averaged time series presenting the joint moments about the ML axis of the left and right hip, knee and ankle from TOR until the second HSR. Each subfigure contains the results for perturbations given at TOR (top graphs), MS (middle graphs), and HSR (bottom graphs). The shaded area indicates the duration the perturbation was given. The unperturbed condition is presented in gray together with the standard deviation, FPP are presented in blue and BPP in red. The graphs are time synchronised at each gait event.

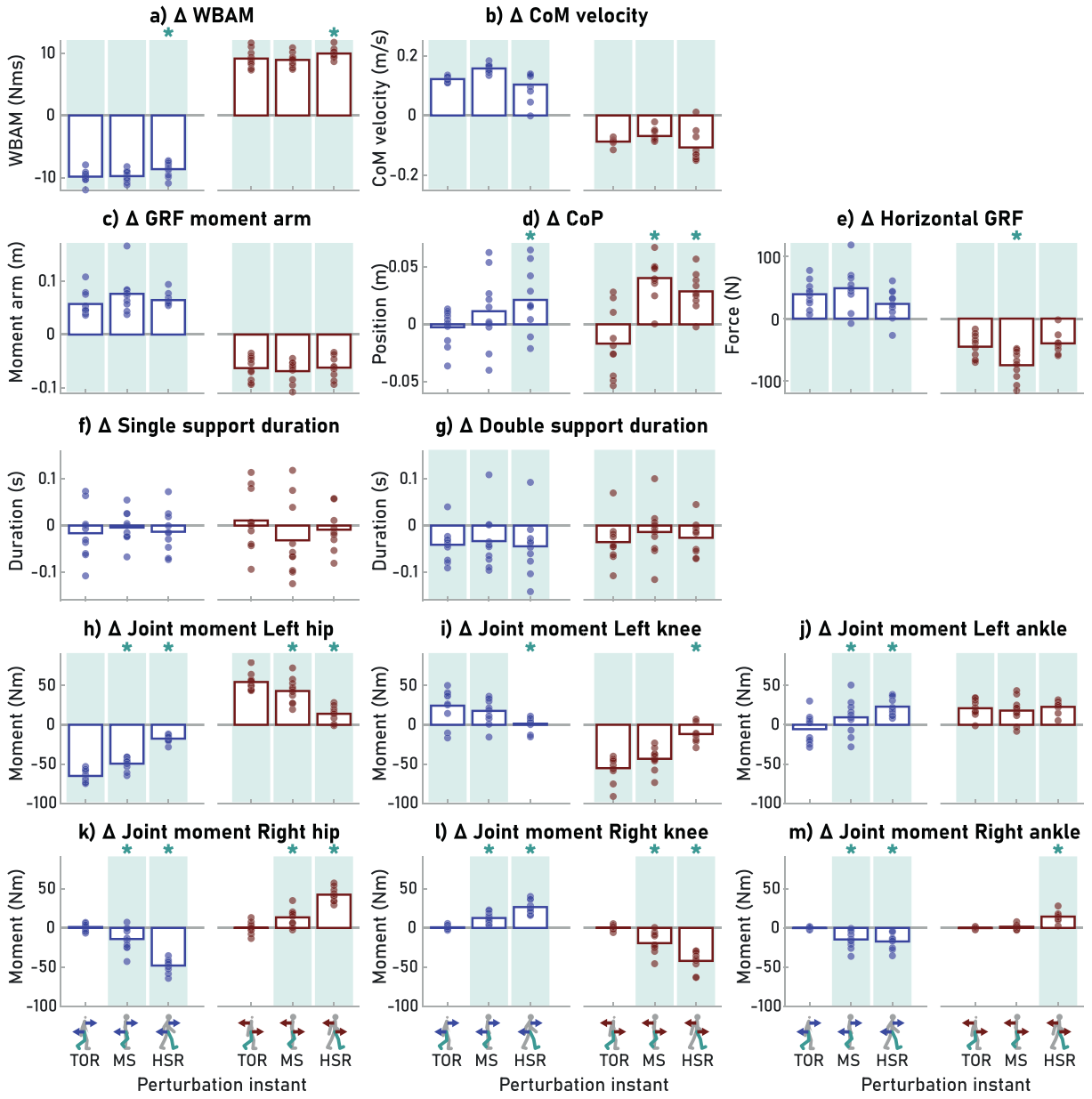

Fig. 4. Maximal deviations outcome measures. Bar plots presenting the maximum deviations of the outcome measures with respect to the unperturbed condition within the first 0.3 s after the perturbation onset (and 0.16 s for WBAM), together with the results of the statistical tests. FPP are presented in blue and BPP in red. The area behind the bar is shaded if there is a significant effect of the perturbation condition on the outcome measure, based on the linear mixed model ($p < 0.05$), and/or additional t-test ($p < 0.005$). A * is presented below the bar if the outcome due to the perturbation at that instant significantly differs from those after the other perturbation instants (based on the linear mixed model, $p < 0.05$). The dots show the results of the individual participants. For the position measures a positive value means a more forward/anterior position with respect to baseline. For the joint moments a positive value means larger flexion/dorsiflexion moment or a smaller extension/plantarflexion moment with respect to baseline.

4. Discussion

The aim of this study was to find whether the balance response to WBAM perturbations given during very slow walking depends on the instant of the gait cycle at which the perturbation is given. We showed that the GRF moment arm needed for the recovery did not change due to the perturbation instant. However, the perturbation onset did effect the contributions of the CoP and/or GRF modulation to the GRF moment arm modulation. For the BPP the observed CoP modulation was not according our hypothesis, since these modulations would theoretically counteract the required WBAM recovery.

As hypothesized for the FPP the perturbation instant affected the contribution from the CoP modulation to the recovery. For the FPP given at MS a trend was shown for a more forward positioned CoP contributing to a GRF passing in front of the CoM and for the perturbations given at HSR this effect was significant. However, this effect was not as strong as expected, because after FPP at MS the recovery could benefit from a more anterior CoP (Zadravec et al., 2020; van den Bogaart, Bruijn, van Dieën, & Meyns, 2020). One of the reasons for this could be the limited time between the perturbation onset and the following HSR hindering a large CoP modulation by foot placement (Vlutters et al., 2018; Leestma et al., 2023). The FPP did not affect the single support duration, but the double support duration was significantly decreased for all perturbation instants. Our data presented an early weight shift during double support which could have caused this effect, bringing the CoP more forward earlier during this gait phase (van Mierlo et al., 2021; van Mierlo, Ormiston, Vlutters, van Asseldonk, & van der Kooij, 2023). For all perturbation instants a larger forward GRF was present contributing to the GRF passing in front of the CoM. While there was no significant effect of the perturbation instant, it seemed that a smaller change was present after perturbations given at HSR. Probably because of the contributing CoP modulation, a smaller change in the horizontal GRF sufficed (Zadravec et al., 2020; van den Bogaart et al., 2020).

After the BPP the response did not occur as expected. For the perturbations given at MS and HSR the peak CoP position was significantly more forward. This is a CoP modulation that does not assist in recovering the WBAM, and even counteracts it. Therefore, it required the more extreme horizontal GRF modulations in order to have the GRF passing posterior to the CoM. For the BPP given at MS it seems that for most participants this anterior position of the CoP originates from an early HSR, indicated by the decreased single support duration. This early HSR appears to be counter-intuitive for a BPP. However at MS, the instant of the perturbation, the swing leg is close to the floor, possibly causing this early and quick foot placement. This early foot placement is not directly assisting in the WBAM recovery, therefore it can be questioned why this is happening and where it originates from. Since changes in foot placement after perturbations due to voluntary actions usually show response times larger than 150 ms (Reimann et al., 2017; Vlutters et al., 2018; Hof et al., 2010; Hof & Duysens, 2013), it probably has an involuntary cause, such as a reflex or direct mechanical effect.

Although not so extreme as for the perturbations given at MS, also after BPP given at HSR the CoP was placed more anterior. This could be explained by an early load shift from the trailing leg towards the leading leg during double support, however it is unclear why this is done. The time series show that during the following single support right the CoP is actually placed more posterior with respect to the CoM, assisting in obtaining the GRF moment arm needed for recovering WBAM. Overall it seems that for the BPP the initial response in CoP modulation is quite strong with respect to the other perturbation instants and not directly supporting the WBAM recovery. However, the response that is following afterwards actually assists in the recovery. Since we are looking at the peak deviation in the outcome measures, this effect is not being captured in the statistics, but it is visible in the time series.

Considering the joint contributions to the balance recovery, as expected a clear shift occurred from the left (trailing) toward the right (leading) leg for perturbations given during MS or HSR with respect to those given at TOR. This makes sense because the main contribution will come from the stance leg. Since the recovery of the WBAM perturbations is done within the swing phase for the perturbations given at TOR, the right leg did not need to contribute anymore after HSR. For the perturbations given at MS or HSR, the right leg did significantly contribute. At the same time the contribution of the left leg decreased, especially when perturbations were given at HSR. From the instant an actual joint response was present, most of the load was already shifted towards the leading leg.

We would like to mention is that the results suggest a significant effect of our perturbations on the WBLM. However, we would like to handle these results carefully since the presented CoM velocity changes are not being reflected in the total horizontal force including the horizontal GRF and interaction forces between the motors and the participant. The CoM velocity changes occur before the horizontal forces indicates a change of the CoM velocity and the interaction forces between the motor and the participant would even suggest a CoM velocity the other way around. The use of a rigid upper body model in OpenSim could have caused an overestimation of the CoM displacement resulting in this effect, a similar effect observed and explained in our previous study (van Mierlo et al., 2022).

Daily-life balance perturbations can occur at every instant of the gait cycle. Our work presents insights into the understanding and generalization of human balance recovery responses throughout the gait cycle. This is an important aspect considering the development of assistive devices supporting balance in daily-life or balance specific rehabilitation goals. However, we should keep in mind that these results are fundamental and that this study was performed with a group of young and healthy individuals walking very slowly. Additional research is needed to see how this translates to those with balance related issues due to a movement disorder or aging, since they might not be able to produce similar recovery strategies as the healthy participants presented in our study (Liu, McNitt-Gray, & Finley, 2022). Another translation that should be made in the step towards daily-life balance recovery is the check on how the balance strategies after controlled balance perturbations during treadmill walking relate to those being encountered in daily practice when certain perturbations cause changes in the WBAM.

4.1. Conclusion

During very slow walking, the instant of the gait cycle at which a perturbation of the WBAM is given does not affect the GRF moment arm modulation needed to counteract the perturbation, but it does affect the way the GRF moment arm modulation is achieved. The used CoP and GRF modulation for achieving this varies among the various perturbation onset instants and directions.

CRediT authorship contribution statement

M. van Mierlo: Conceptualization, Methodology, Investigation, Software, Formal-analysis, Writing-original-draft, Visualization. **M. Abma:** Conceptualization, Methodology, Investigation. **M. Vlutters:** Conceptualization, Methodology, Software, Writing-review-editing. **E.H.F. van Asseldonk:** Conceptualization, Methodology, Writing-review-editing, Supervision, Project-administration,

Funding-acquisition. **H. van der Kooij:** Conceptualization, Methodology, Writing-review-editing, Supervision, Project-administration, Funding-acquisition.

Declaration of Competing Interest

The authors declare that they have no known competing financial interests or personal relationships that could have appeared to influence the work reported in this paper.

Data availability

The data used for this study is published on 4TU. ResearchData and can be found via the following DOI: 10.4121/37b4bfd6-5194-4f89-a968-5fa0d74811ec.

Acknowledgements

This work is part of the research program Wearable Robotics with project number P16-05, which is (partly) funded by the Dutch Research Council (NWO).

Appendix A. Results statistical analysis

Table A1
Tables presenting the results of the statistical analysis. For each outcome measure, WBAM (about ML axis), CoM velocity (in AP direction), GRF moment arm (in sagittal plane), CoP position (in AP direction), horizontal GRF, gait phase durations of the single and double support, and the joint moments of the left and right hip, knee and ankle (about ML axis), the results are shown for parameter estimate values (Par) and p-values (p) of the fixed effects (Intercept, Onset MS and Onset HSR) of the linear mixed model, together with the overall marginal- and conditional R^2 values of the model fit. The intercept coincides with the perturbation onset at TOR. The t-value (t), degrees of freedom (df), and p-value (p) results of the additional t-tests are presented in the extra column in case these tests were performed. The left column presents the results for the FPP and the right column for the BPP.

	Whole-body angular momentum (N m s)					
	Forward pitch perturbations			**Backward pitch perturbations**		
Fixed effect	**Parameter**	**p-value**	**T-test t(df), p**	**Parameter**	**p-value**	**T-test t(df), p**
Intercept	−9.85	<0.001		9.17	<0.001	
Onset MS	0.08	0.739		−0.22	0.377	
Onset HSR	1.21	<0.001	−23(9), <0.001	0.66	0.016	
Model fit	R^2-marginal 0.24; R^2-conditional 0.77			R^2-marginal 0.10; R^2-conditional 0.80		
	CoM velocity (m s^{-1})					
	Forward pitch perturbations			**Backward pitch perturbations**		
Fixed effect	**Parameter**	**p-value**	**T-test t(df), p**	**Parameter**	**p-value**	**T-test t(df), p**
Intercept	0.168	<0.001		−0.151	<0.001	
Onset MS	0.009	0.312		0.015	0.231	
Onset HSR	−0.003	0.718		0.008	0.544	
Model fit	R^2-marginal 0.03; R^2-conditional 0.65			R^2-marginal 0.03; R^2-conditional 0.38		
	GRF moment arm (m)					
	Forward pitch perturbations			**Backward pitch perturbations**		
Fixed effect	**Parameter**	**p-value**	**T-test t(df), p**	**Parameter**	**p-value**	**T-test t(df), p**
Intercept	0.057	<0.001		−0.063	<0.001	
Onset MS	0.019	0.061		−0.006	0.362	
Onset HSR	0.07	0.456		0.002	0.762	
Model fit	R^2-marginal 0.10; R^2-conditional 0.28			R^2-marginal 0.03; R^2-conditional 0.54		
	CoP position (m)					
	Forward pitch perturbations			**Backward pitch perturbations**		
Fixed effect	**Parameter**	**p-value**	**T-test t(df), p**	**Parameter**	**p-value**	**T-test t(df), p**
Intercept	−0.003	0.749		−0.017	0.018	
Onset MS	0.014	0.155		0.057	<0.001	7.1(9), <0.001

(*continued on next page*)

Table A1 (*continued*)

Onset HSR	0.024	0.020		0.046	<0.001	5.1(8), <0.001
Model fit	R^2-marginal 0.14; R^2-conditional 0.37			R^2-marginal 0.59; R^2-conditional 0.64		

Horizontal GRF (N)

	Forward pitch perturbations			Backward pitch perturbations		
Fixed effect	**Parameter**	**p-value**	**T-test t(df), p**	**Parameter**	**p-value**	**T-test t(df), p**
Intercept	39.3	<0.001		−45.2	<0.001	
Onset MS	9.7	0.352		−29.8	<0.001	−9.8(9), <0.001
Onset HSR	−15.6	0.140		6.9	0.241	
Model fit	R^2-marginal 0.14; R^2-conditional 0.36			R^2-marginal 0.41; R^2-conditional 0.77		

Single support duration (ms)

	Forward pitch perturbations			Backward pitch perturbations		
Fixed effect	**Parameter**	**p-value**	**T-test t(df), p**	**Parameter**	**p-value**	**T-test t(df), p**
Intercept	−1.6	0.254		1.1	0.592	
Onset MS	−0.4	0.226		−3.2	0.070	
Onset HSR	−1.3	0.753		−1.3	0.307	
Model fit	R^2-marginal 0.01; R^2-conditional 0.75			R^2-marginal 0.07; R^2-conditional 0.43		

Double support duration (ms)

	Forward pitch perturbations			Backward pitch perturbations		
Fixed effect	**Parameter**	**p-value**	**T-test t(df), p**	**Parameter**	**p-value**	**T-test t(df), p**
Intercept	−4.1	0.018		−3.6	0.020	
Onset MS	−3.3	0.704		−1.4	0.202	
Onset HSR	−4.5	0.871		−2.7	0.636	
Model fit	R^2-marginal 0.01; R^2-conditional 0.23			R^2-marginal 0.04; R^2-conditional 0.36		

Joint moment Left hip (N m)

	Forward pitch perturbations			Backward pitch perturbations		
Fixed effect	**Parameter**	**p-value**	**T-test t(df), p**	**Parameter**	**p-value**	**T-test t(df), p**
Intercept	−65.2	<0.001		54.6	<0.001	
Onset MS	15.6	<0.001	−19.6(9), <0.001	−11.5	0.010	8.5(9), <0.001
Onset HSR	47.5	<0.001	−11.1(9), <0.001	−41.4	<0.001	4.2(8), 0.003
Model fit	R^2-marginal 0.90; R^2-conditional 0.91			R^2-marginal 0.68; R^2-conditional 0.82		

Joint moment Right hip (N m)

	Forward pitch perturbations			Backward pitch perturbations		
Fixed effect	**Parameter**	**p-value**	**T-test t(df), p**	**Parameter**	**p-value**	**T-test t(df), p**
Intercept	1.1	0.723		0.1	0.961	
Onset MS	−15.3	0.001		13.3	0.010	
Onset HSR	−49.1	<0.001		42.0	<0.001	
Model fit	R^2-marginal 0.82; R^2-conditional 0.84			R^2-marginal 0.79; R^2-conditional 0.84		

Joint moment Left knee (N m)

	Forward pitch perturbations			Backward pitch perturbations		
Fixed effect	**Parameter**	**p-value**	**T-test t(df), p**	**Parameter**	**p-value**	**T-test t(df), p**
Intercept	24.4	<0.001		−55.3	<0.001	
Onset MS	−6.6	0.176		12.0	0.030	
Onset HSR	−23.0	<0.001	0.5(9), 0.626	44.0	<0.001	−3.1(8), 0.015
Model fit	R^2-marginal 0.27; R^2-conditional 0.69			R^2-marginal 0.65; R^2-conditional 0.76		

Joint moment Right knee (N m)

	Forward pitch perturbations			Backward pitch perturbations		
Fixed effect	**Parameter**	**p-value**	**T-test t(df), p**	**Parameter**	**p-value**	**T-test t(df), p**
Intercept	0.7	0.716		0.4	0.898	
Onset MS	11.9	<0.001		−19.8	<0.001	
Onset HSR	25.9	<0.001		−42.5	<0.001	
Model fit	R^2-marginal 0.75; R^2-conditional 0.82			R^2-marginal 0.74; R^2-conditional 0.82		

(*continued on next page*)

Table A1 (*continued*)

	Joint moment Left ankle (N m)					
	Forward pitch perturbations			Backward pitch perturbations		
Fixed effect	**Parameter**	**p-value**	**T-test t(df), p**	**Parameter**	**p-value**	**T-test t(df), p**
Intercept	−5.6	0.322		21.1	<0.001	
Onset MS	−15.2	0.039		−3.0	0.469	
Onset HSR	28.7	<0.001		1.7	0.691	
Model fit	R^2-marginal 0.27; R^2-conditional 0.69			R^2-marginal 0.65; R^2-conditional 0.76		

	Joint moment Right ankle (N m)					
	Forward pitch perturbations			Backward pitch perturbations		
Fixed effect	**Parameter**	**p-value**	**T-test t(df), p**	**Parameter**	**p-value**	**T-test t(df), p**
Intercept	−0.2	0.949		−0.2	0.885	
Onset MS	−14.5	<0.001		1.7	0.365	
Onset HSR	−17.1	<0.001		14.6	<0.001	
Model fit	R^2-marginal 0.32; R^2-conditional 0.48			R^2-marginal 0.03; R^2-conditional 0.42		

References

Delp, S. L., Anderson, F. C., Arnold, A. S., Loan, P., Habib, A., John, C. T., et al. (2007). Opensim: Open-source software to create and analyze dynamic simulations of movement. *IEEE Transactions on Biomedical Engineering, 54*, 1940–1950. https://doi.org/10.1109/TBME.2007.901024

Eveld, M. E., King, S. T., Vailati, L. G., Zelik, K. E., & Goldfarb, M. (2021). On the basis for stumble recovery strategy selection in healthy adults. *Journal of Biomechanical Engineering, 143*. https://doi.org/10.1115/1.4050171

Forner Cordero, A., Koopman, H. F. J. M., & van der Helm, F. C. T. (2003). Multiple-step strategies to recover from stumbling perturbations. *Gait and Posture, 18*, 47–59. https://doi.org/10.1016/S0966-6362(02)00160-1

Golyski, P. R., Vazquez, E., Leestma, J. K., & Sawicki, G. S. (2022). Onset timing of treadmill belt perturbations influences stability during walking. *Journal of Biomechanics, 130*. https://doi.org/10.1016/j.jbiomech.2021.110800

Herr, H., & Popovic, M. (2008). Angular momentum in human walking. *Journal of Experimental Biology, 211*, 467–481. https://doi.org/10.1242/jeb.008573

Hof, A. L., & Duysens, J. (2013). Responses of human hip abductor muscles to lateral balance perturbations during walking. *Experimental Brain Research, 230*, 301–310. https://doi.org/10.1007/s00221-013-3655-5

Hof, A. L., Vermerris, S. M., & Gjaltema, W. A. (2010). Balance responses to lateral perturbations in human treadmill walking. *The Journal of Experimental Biology, 213*, 2655–2664. https://doi.org/10.1242/jeb.042572

Leestma, J. K., Golyski, P. R., Smith, C. R., Sawicki, G. S., & Young, A. J. (2023). Linking whole-body angular momentum and step placement during perturbed human walking. *Journal of Experimental Biology, 226*. https://doi.org/10.1242/jeb.244760

Liu, C., McNitt-Gray, J. L., & Finley, J. M. (2022). Impairment in the mechanical effectiveness of reactive balance control strategies during walking in people post-stroke. *Frontiers in Neurology, 13*. https://doi.org/10.3389/fneur.2022.1032417

Matjacic, Z., Zadravec, M., & Olenšek, A. (2020). Biomechanics of in-stance balancing responses following outward-directed perturbation to the pelvis during very slow treadmill walking show complex and well-orchestrated reaction of central nervous system. *Frontiers in Bioengineering and Biotechnology, 8*. https://doi.org/10.3389/fbioe.2020.00884

Millard, M., Wight, D., McPhee, J., Kubica, E., & Wang, D. (2009). Human foot placement and balance in the sagittal plane. *Journal of Biomechanical Engineering, 131*, 1–7. https://doi.org/10.1115/1.4000193

Negishi, T., & Ogihara, N. (2023). Regulation of whole-body angular momentum during human walking. *Scientific Reports, 13*. https://doi.org/10.1038/s41598-023-34910-5

Nymark, J. R., Balmer, S. J., Melis, E. H., Edward, D., & Millar, S. (2005). Electromyographic and kinematic nondisabled gait differences at extremely slow overground and treadmill walking speeds. *Journal of Rehabilitation Research and Development, 42*, 523–534. https://doi.org/10.1682/JRRD.2004.05.0059

R Core Team. (2021). *R: A language and environment for statistical computing*.

Rácz, K., & Kiss, R. M. (2021). Marker displacement data filtering in gait analysis: A technical note. *Biomedical Signal Processing and Control, 70*. https://doi.org/10.1016/j.bspc.2021.102974

Rajagopal, A., Dembia, C. L., Demers, M. S., Delp, D. D., Hicks, J. L., & Delp, S. L. (2016). Full body musculoskeletal model for muscle-driven simulation of human gait. *IEEE Transactions on Biomedical Engineering, 63*, 2068–2079. https://doi.org/10.1109/TBME.2016.2586891

Reimann, H., Fettrow, T. D., Thompson, E. D., Agada, P., McFadyen, B. J., & Jeka, J. J. (2017). Complementary mechanisms for upright balance during walking. *PLoS ONE, 12*, 1–16. https://doi.org/10.1371/journal.pone.0172215

Robert, T., Bennett, B. C., Russell, S. D., Zirker, C. A., & Abel, M. F. (2009). Angular momentum synergies during walking. *Experimental Brain Research*, 185–197. https://doi.org/10.1007/s00221-009-1904-4

Schumacher, C., Berry, A., Lemus, D., Rode, C., Seyfart, A., & Vallery, H. (2019). Biarticular muscles are most responsive to upper-body ptich perturbations in human standing. *Scientific Reports, 9*. https://doi.org/10.1038/s41598-019-50995-3

van den Bogaart, M., Bruijn, S. M., van Dieën, J. H., & Meyns, P. (2020). The effect of anteroposterior perturbations on the control of the center of mass during treadmill walking. *Journal of Biomechanics, 103*. https://doi.org/10.1016/j.jbiomech.2020.109660

van der Kooij, H., Fricke, S. S., van t'Veld, R. C., Vallinas Prieto, A., Keemink, A. Q. L., Schouten, A. C., et al. (2022). Identification of hip and knee joint impedance during the swing phase of walking. *IEEE Transactions on Neural Systems and Rehabilitation Engineering, 30*, 1203–1212. https://doi.org/10.1109/TNSRE.2022.3172497

van Mierlo, M., Vlutters, M., van Asseldonk, E. H. F., & van der Kooij, H. (2021). Centre of pressure modulations in double support effectively counteract anteroposterior perturbations during gait. *Journal of Biomechanics, 126*, Article 110637. https://doi.org/10.1016/j.jbiomech.2021.110637

van Mierlo, M., Ambrosius, J. I., Vlutters, M., van Asseldonk, E. H. F., & van der Kooij, H. (2022). Recovery from sagittal-plane whole body angular momentum perturbations during walking. *Journal of Biomechanics, 141*, Article 111169. https://doi.org/10.1016/j.jbiomech.2022.111169

van Mierlo, M., Ormiston, J. A., Vlutters, M., van Asseldonk, E. H. F., & van der Kooij, H. (2023). Pelvis perturbations in various directions while standing in staggered stance elicit concurrent responses in both the sagittal and frontal plane. *PLoS ONE, 18*. https://doi.org/10.1371/journal.pone.0272245

van Mierlo, M., Vlutters, M., van Asseldonk, E. H. F., & van der Kooij, H. (2023). Sagittal-plane balance perturbations during very slow walking: Strategies for recovering linear and angular momentum. *Journal of Biomechanics, 152*. https://doi.org/10.4121/21370095

Vlutters, M., van Asseldonk, E. H. F., & van der Kooij, H. (2018). Lower extremity joint-level responses to pelvis perturbation during human walking. *Scientific Reports, 8*, 14621. https://doi.org/10.1038/s41598-018-32839-8

Weerdesteyn, V., Laing, A. C., & Robinovitch, S. N. (2012). The body configuration at step contact critically determines the successfulness of balance recovery in response to large backward perturbations. *Gait and Posture, 35*, 462–466. https://doi.org/10.1016/j.gaitpost.2011.11.008

Wu, A. R., Simpson, C. S., van Asseldonk, E. H. F., van der Kooij, H., & Ijspeert, A. J. (2019). Sagittal-plane balance perturbations during very slow walking: Strategies for recovering linear and angular momentum. *Mechanics of Very Slow Human Walking, 9*. https://doi.org/10.1038/s41598-019-54271-2

Zadravec, M., Olenšek, A., Rudolf, M., Bizovicar, N., Goljar, N., & Matjacic, Z. (2020). Assessment of dynamic balancing responses following perturbations during slow walking in relation to clinical outcome measures for high-functioning post-stroke subjects. *Journal of NeuroEngineering and Rehabilitation, 17*. https://doi.org/10.1186/s12984-020-00710-5